VOL. 10, NO. 17, SEPTEMBER 2015 ISSN 1819-6608
ARPN Journal of Engineering and Applied Sciences


www.arpnjournals.com

PHYSICAL STUDIES ON ELECTROLESS NI-YSZ COMPOSITE COATING

N. Bahiyah Babaa and S. Noorazuani Abd Lahli
Faculty of Manufacturing Engineering Technology, TATI University College, Kemaman, Terengganu, Malaysia
E-Mail: bahiyah@tatiuc.edu.my

ABSTRACT

The paper discussed on the physical properties of the electroless Ni-YSZ composite coating. The main properties of concern are the ceramic YSZ to metallic Ni ratio as well as the porosity content within the coating. The composition of YSZ in the composite coating is the reinforcement for the composite coating. The composition was measured via SEM/EDXA and matrix digestion method (ASTM D3171). The amount of porosity in the composite coating was measured using Archimedes density (ASTM D792). Three batches of sample were compared with various types of pore former namely activated carbon, graphite and starch. Nanoindentation was carried out to determine the hardness of the composite coating between the three batches of samples. The SEM micrographs of Ni-YSZ composite coating for the three batches at 5k magnifications coupled with EDX analysis was discussed together with the XRD analysis.

Keywords: electroless nickel, composite coating, ni-ysz, pore former, porosity.

INTRODUCTION

Nickel ceramic composite is well known in engineering as it combines nickel (Ni) that is very well known for its high thermal, high electronic conductivity and high corrosion resistance, with yttria-stabilised zirconia (YSZ) for its high ionic conductivity, high impact and hardness strength. These properties combination made nickel composite coating a highly demand especially for corrosion wear and thermal resistance as well as the solid oxide fuel cell anode [1-5]. The property of composites mostly depends on the ratio of reinforcement and matrix as well as the reinforcement orientation. Hence, the composition of Ni and YSZ in the coating deposition can be controlled to produce desired properties. It is desirable to have high ceramic YSZ to metallic Ni ratio as higher ceramic content endures high corrosion, thermal and wear resistance. Varying ceramic YSZ coating in the composite has an advantage in which a gradient of coating layers with increasing ceramic content inside to outside for heat and corrosion resistance respectively [6-10]. The Ni-YSZ composite coating was fabricated by electroless nickel co-deposition process. This is a single fabrication method consists of an in-situ incorporation of inert ceramic particles in the conventional Ni-P matrix [7, 11, 12]. Electroless deposition has been extensively applied in industry and the most prevalent coating offers excellent corrosion, wear and abrasion resistance, ductility, lubricity, electrical properties, and high hardness [13]. The incorporation of particles in electroless deposit has been widely investigated and these include the incorporation of diamond, silicon carbide, silicon nitride, silicon oxide, boron carbide, alumina, ceria, yttria and zirconia particles [14-16]. Typical co-deposition consists of particulates in the size range of 0.1-10 μm with loading of up to 40% volume of the total matrix [15]. The electroless nickel deposition has excellent uniformity and dense deposition with thickness less than 10 μm [6, 13, 17, 18]. Studies showed that certain porosity level in the deposition is critical as the amount of porosity enhanced thermal insulation for thermal barrier coatings and gas circulation in fuel cell anode applications [16, 19]. Adequate amount of porosity required is in the range of 30-40%. It is found that the amount of porosity in the coating should not exceed 40 vol. % as greater amount reduces the mechanical properties of the deposit. Thus, an adequate amount of porosity and reasonable mechanical properties should be balance. Studies found that the amount of porosity in electroless nickel deposition could be induced by varying the agitation methods, deposition rate, bath pH, substrate surface condition and incorporate pore former.

EXPERIMENTAL SETUP

Materials and Preparation

Ceramic substrate of alumina tiles (Beihai Ltd., China) as the base for the composite deposition was used. The substrate has manufacturer standard dimension of 30x30x1 mm. 8%YSZ powders of 2 μm particles size (TOSOH, Japan) was incorporated in the electroless bath ranges between 15-25g. Three types of pore former namely graphite powder, activated carbon and starch were included.

Electroless Nickel Deposition

The ceramic alumina substrate was sensitized to activate the surface. All non-proprietary solutions were prepared using AR grade chemicals and high purity deionised water. After the pre-treatment process sequence listed in Table-1, the electroless nickel composite deposition of Ni-YSZ was performed within 3 hours to minimize effects of chemical degradation. The electroless nickel chemicals produced a bright mid-phosphorous (6-9%) nickel deposit. The solution was heated and maintained at 89 ± 2 ^{0}C using a hotplate (IKA 3581200). Appropriate bath agitation was required to keep the ceramic powders suspended in the bath. The coating time was kept constant at 60 minutes.

Table-1. Electro less nickel co-deposition process.

Trade name	Soaking Time	Temperature
Cuprolite X96DP	15 min	60°C
Uniphase PHP Pre-catalyst	15 min	20°C
Uniphase PHP Catalyst	15 min	40°C
Niplast AT78	15 min	40°C
Electroless Nickel SLOTONIP 1850	60 min	89°C

Addition of pore former at designated weight was included along with the 8YSZ powders. There are 3 batches of samples namely Ni-YSZ composite coating with activated carbon (EN-C), graphite (EN-G) and starch (EN-S). After coating, all samples were heated in oven at 700-750 ^{0}C for 1 hour.

Matrix Digestion

This test physically removed the matrix by digestion method (ASTM D3171). The remaining reinforcement content by weight or volume percent obtained. The Ni composition was digested by 70% of Nitric Acid (HNO_3). The solution was heated up to the temperature ranges 40-50 ^{0}C using hotplate (IKA 3581200). The maximum time for digestion was 6 hour. The matrix was considered fully digested as no trace of the reinforcement laminates combination remains. Filter the remaining content of digestion was filtered by filter pump and placed in an oven at 100 °C to dry. The weight percent of 8YSZ can be calculated by determining initial mass of the specimen and final mass of the specimen after digestion or combustion as in Eqn. (1):

$$W_f = \frac{M_f}{M_i} \times 100 \quad (1)$$

where M_i = Initial mass and M_f = Final mass

Archimedes Density

Archimedes specific density was used to measure porosity fraction in sample. The basic Archimedes principle states that the amount of displaced water volume was equal to the immersed object volume. The determination of the solid substance density can be done by buoyancy or displacement methods from ASTM D792. Then, porosity fraction, f_p can be calculated by determining the difference between unity and the fraction of bulk and true density as described in Eqn. (2) [20]:

$$f_p = \frac{\rho_t - \rho_b}{\rho_t} = 1 - \frac{\rho_b}{\rho_t} \quad (2)$$

where ρ_b = Bulk Density and ρ_t = True Density

SEM-EDX & XRD

The nickel composition was measured using Scanning Electron Microscope (SEM) coupled with Energy Dispersive X-ray Analysis (EDXA). The acceleration voltage was 15 kV. The EDX expose time was kept constant at 300 s and expose area was kept constant. The element and compound in the composite coatings were analysed by X-ray diffraction (XRD).

Nanoindentation

Nanoindentation analysis (CSIRO, Australia) are intended for hardness measurements of thin surface coatings. The nanoindentation is used to perform accurate result under various load range from 10 mN up to 5 N. For each loading or unloading cycle, the applied load value and indenter displacement are recorded in situ to obtain the indentation hysteresis curves.

RESULTS AND DISCUSSION

Electroless Ni-YSZ Composition

The properties of the composite strongly depend on the reinforcement content. The amount of reinforcement included in the composite coating was measured by SEM/EDXA and matrix digestion method. Figure-1 shows variation of YSZ content in the Ni-YSZ composite coating for EN-C, EN-G and EN-S by SEM/EDXA and matrix digestion method.

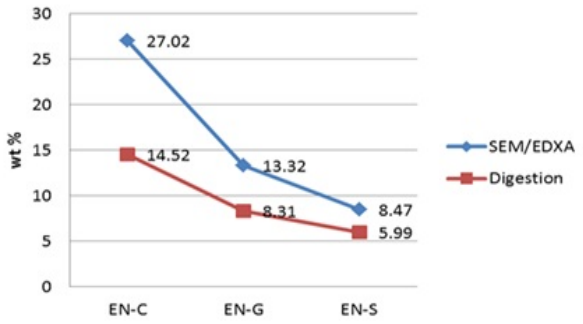

Figure-1. Comparison of 8YSZ composition via SEM/EDXA and digestion method.

The results show that the descending trend of YSZ composition starting from EN-C followed by EN-G and EN-S obtained by SEM/EDXA and matrix digestion methods. The composition obtained by SEM-EDXA was higher than matrix digestion method due to the fact that SEM/EDXA was concentrated on the surface and specific area. The matrix digestion method represents the true composition of ceramic YSZ. However, during the process there is a possibility that some of the YSZ powders were left uncollected. Hence, the results obtained by matrix digestion method were lower compared to the SEM/EDXA.

Electroless Ni-YSZ Characterization

The electroless Ni-YSZ composite coating was analysed using SEM/EDXA. The corresponding EDX spectrum is given in Figure-2 shows the presence of major peak of nickel (Ni), zirconium (Zr), sodium (Na), carbon (C), oxygen (O) and phosphorous (P). These confirmed that the composites were composed of combination of metallic nickel and ceramic YSZ. The existence of element P in the composite was due to the fact that P is one of the major elements in the electroless hypophosphite-based bath solution.

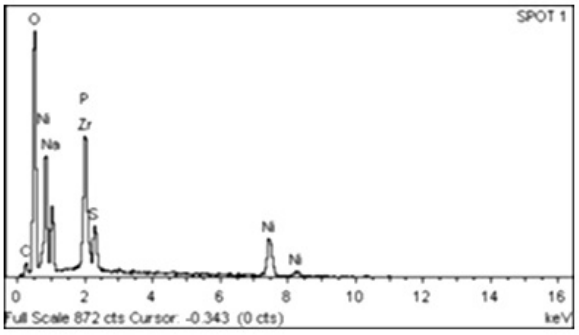

Figure-2. EDX spectrum of electroless Ni-YSZ composite coating.

SEM micrograph of the three batches of electroless Ni-YSZ composite coating is shown in Figure-3. Generally, the white areas represent the YSZ ceramic, the grey areas were the metallic nickel matrix and the dark areas were the porosity. The surface appears highly porous in the EN-S samples compared to EN-C and EN-G. This observation due to the properties of starch which tends to gelled upon heating in aqueous solution. The gelled in and on the coating and upon heating leaving the uneven lump. Comparing EN-C and EN-G, it was observed that EN-C shows rougher surface and higher black areas. Even both activated carbon and graphite are originally from the same group, activated carbon was highly porous and softer in nature thus it is easier to absorb and blend-in the solution and embedded in the coating. Hence, upon heating the activated carbon evaporated leaving empty spaces or porosity. There was a very fine crack on the surface of EN-G sample. This might arise due to the different in thermal expansion coefficient of the ceramic YSZ and the metallic Ni.

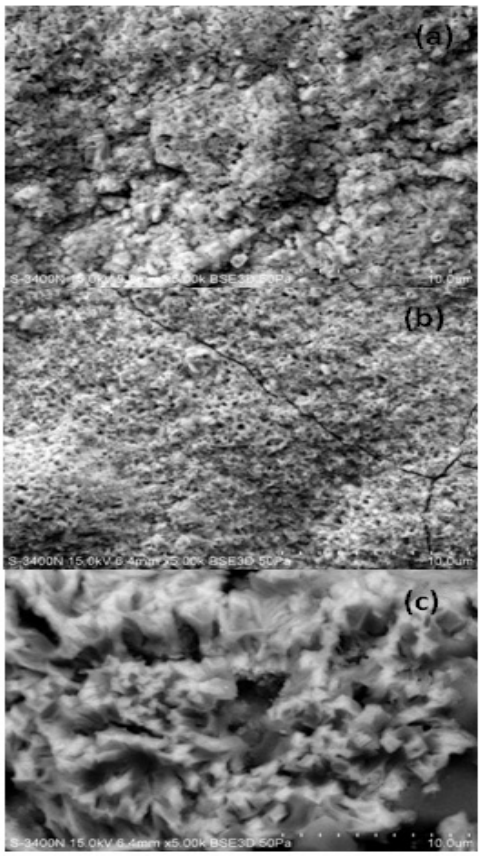

Figure-3. SEM micrograph at 5k magnification of Ni-YSZ composite coatings (a) EN-C (b) EN-G (c) EN-S.

The corresponding XRD analysis given in Figure-4 shows the major compound of nickel oxide followed by alumina. Alumina was detected as the substrate of the coating was the alumina tile. The Ni-YSZ composite coating has a thickness approximately 10-20 μm, thus it is possible for the X-ray radiation to penetrate beneath the Ni-YSZ coating to the surface of substrate (Al_2O_3).

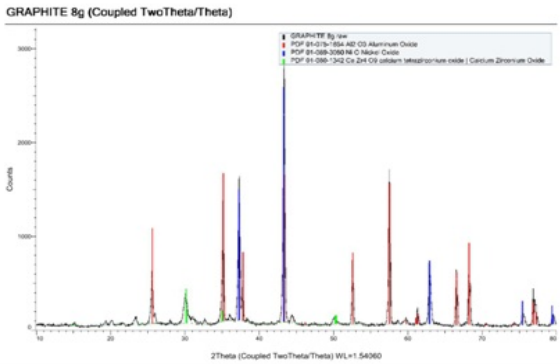

Figure-4. XRD diffraction peaks for Ni-YSZ composite coating.

Electroless Ni-YSZ Physical Properties

The literature stated that the amount of porosity should not be more than 40 vol. % as not to affect the mechanical properties of the coating. The porosity of Ni-YSZ composite coating was measured by Archimedes density as shown in Figure-5. It was observed that the % of fraction porosity for EN-S was the highest at 59.7% compared to the activated carbon and graphite. This observation was supported the analysis done by the SEM micrograph in the previous section. The hardness of the Ni-YSZ composite coating was measured using the nanoindentation due to a very thin coating surface. There were 3 runs of test for each samples and was tabulated in Table-2. It was found that EN-C and EN-G hardness were not very much differed to the EN-S. The observation was due to the fact that EN-S contain high amount of porosity compared to the other two samples, EN-C and EN-G.

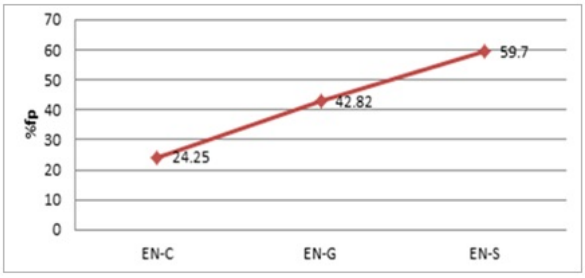

Figure-5. Porosity analysis of Archimedes density measurement.

Table-2. Nanoindentation test for Ni-YSZ composite coating.

Nanoindentation [Hv]	EN-C	EN-G	EN-S
Run1	24.016	30.898	19.866
Run2	28.374	29.404	18.619
Run3	28.374	32.117	17.825
Average :	26.921	30.806	18.770

CONCLUSIONS

The composition of electroless Ni-YSZ composite coating measured by SEM/EDXA and matrix digestion showed similar descending trend follow the EN-C, EN-G and EN-S. The SEM/EDXA gave higher values as it was represented certain area and depth whereas the matrix digestion represent the true values. The EDX analysis showed the existence of nickel (Ni), zirconium (Zr), sodium (Na), carbon (C), oxygen (O) and phosphorous (P) elements. Whereas the XRD analysis indicated the major compound of nickel oxide followed by alumina were found. Porosity in the Ni-YSZ composite coating was the highest for the sample with starch incorporation and the lowest for activated carbon incorporation. The amount of porosity seemed to affect the hardness of the Ni-YSZ composite coating which the highest porosity gave the lowest nano hardness value.

ACKNOWLEDGEMENTS

The authors acknowledge the support of Ministry of Higher Education Malaysia for the financial fund under Fundamental Research Grant Scheme (FRGS/1/2012/TK07/TATID2/1).

REFERENCES

[1] Sudagar J., J. Lian and W. Sha. 2013. Electroless nickel, alloy, composite and nano coatings–A critical review. Journal of Alloys and Compounds. Vol. 571, pp. 183-204.

[2] Rabizadeh T. and S.R. Allahkaram. 2011. Corrosion resistance enhancement of Ni–P electroless coatings by incorporation of nano-SiO particles. Materials & Design. Vol. 32, No.1, pp. 133-138.

[3] Baba N.B., A. Davidson and T. Muneer. 2011. YSZ-reinforced Ni-P deposit: an effective condition for high particle incorporation and porosity level. Advanced Materials Research. Vol. 214, pp. 412-417.

[4] Lekka M. *et al.* 2011. Scaling-up of the electrodeposition process of nano-composite coating for corrosion and wear protection. Electrochimica Acta. Vol. 55, No. 27, pp. pp.7876-7883.

[5] Pratihar S.K., A. Dassharma and H.S. Maiti. 2005. Processing microstructure property correlation of porous Ni–YSZ cermets anode for SOFC application. Materials research bulletin. Vol. 40, No.11, pp. 1936-1944.

[6] Adebisi A.A., M.A. Maleque and M.M. Rahman. Metal matrix composite brake rotor: Historical development and product life cycle analysis. International Journal of Automotive and Mechanical Engineering. Vol. 4, pp. 471-480.

[7] Moniruzzaman M. and S. Roy. 2011. Effect of pH on electroless Ni-P coating of conductive and nonconductive materials. International Journal of Automotive and Mechanical Engineering. Vol. 4, pp. 481-489.

[8] Bhaskar H.B. and A. Sharief. 2012. Effect of solutionizing on dry sliding wear of Al2024-Beryl metal matrix composite. Journal of Mechanical Engineering and Sciences. Vol. 3, pp. 281-290.

[9] Hardinnawirda, K. and I. SitiRabiatull Aisha. 2012. Effect of rice husks as filler in polymer matrix composites. Journal of Mechanical Engineering and Sciences. Vol. 2, pp. 181-186.

[10] Ibrahim, M.S., S.M. Sapuan, and A.A. Faieza. 2012. Mechanical and thermal properties of composites

from unsaturated polyester filled with oil palm ash. Journal of Mechanical Engineering and Sciences. Vol. 2, pp. 133-147.

[11] Wang, L., *et al.* 2011. Influence of pores on the thermal insulation behavior of thermal barrier coatings prepared by atmospheric plasma spray. Materials & Design. Vol. 32, No. 1, pp. 36-47.

[12] Moniruzzaman, M., M.M. Rakib, and F.T. Matin. 2012. Cr-Ni alloy electrodeposition and comparison with conventional pure Cr coating technique. International Journal of Automotive and Mechanical Engineering. Vol. 6, pp. 692-700.

[13] Mallory, G.O. and J.B. Hajdu. 1990. Electroless plating: fundamentals and applications. William Andrew.

[14] Zuleta A. *et al.* 2009. Preparation and characterization of electroless Ni–P–Fe3O4 composite coatings and evaluation of its high temperature oxidation behaviour. Surface and Coatings Technology. Vol. 203, No. 23, pp. 3569-3578.

[15] Hung, C., C. Lin, and H.C. Shih. 2008. Tribological studies of electroless nickel/diamond composite coatings on steels. Diamond and Related Materials. Vol. 17, No. 4, pp. 853-859.

[16] Yu X. *et al.* 2000. XPS and AES investigation of two electroless composite coatings. Applied surface science. 2000. Vol. 158, No. 3, pp. 335-339.

[17] Hafizi, Z.M., J. Epaarachchi, and K.T. Lau. 2013. An investigation of acoustic emission signal attenuation for monitoring of progressive failure in fiberglass reinforced composite laminates. International Journal of Automotive and Mechanical Engineering. Vol. 8, pp. 1442-1456.

[18] Haque M.M. *et al.* 2014. Corrosion comparison of galvanized steel and aluminum in aqueous environments. International Journal of Automotive and Mechanical Engineering. Vol. 9, pp. 1758-1767.

[19] Simwonis D. *et al.* 1999. Properties of Ni/YSZ porous cermets for SOFC anode substrates prepared by tape casting and coat-mix® process. Journal of Materials Processing Technology. Vol. 92, pp. 107-111.

[20] Kingery W.D. 1960. Introduction to ceramics.